Enhanced synaptic plasticity in mice with phosphomimetic mutation of the GluA1 AMPA receptor

Yuichi Makino, Richard C. Johnson, Yilin Yu, Kogo Takamiya[1], and Richard L. Huganir[2]

Department of Neuroscience and The Howard Hughes Medical Institute, The Johns Hopkins University School of Medicine, Baltimore, MD 21205

Contributed by Richard L. Huganir, April 11, 2011 (sent for review March 23, 2011)

Phosphorylation of the GluA1 subunit of AMPA receptors has been proposed to regulate receptor trafficking and synaptic transmission and plasticity. However, it remains unclear whether GluA1 phosphorylation is permissive or sufficient for enacting these functional changes. Here we investigate the role of GluA1 phosphorylation at S831 and S845 residues in the hippocampus through the analyses of GluA1 S831D/S845D phosphomimetic knock-in mice. S831D/S845D mice showed normal total and surface expression and subcellular localization of GluA1 as well as intact basal synaptic transmission. In addition, theta-burst stimulation, a protocol that was sufficient to induce robust long-term potentiation (LTP) in WT mice, resulted in LTP of similar magnitude in S831D/S845D mice. However, S831D/S845D mice showed LTP induced with 10-Hz stimulation, a protocol that is weaker than theta-burst stimulation and was not sufficient to induce LTP in WT mice. Moreover, S831D/S845D mice exhibited LTP induced with spike-timing–dependent plasticity (STDP) protocol at a long pre-post interval that was subthreshold for WT mice, although a suprathreshold STDP protocol at a short pre-post interval resulted in similarly robust LTP for WT and S831D/S845D mice. These results indicate that phosphorylation of GluA1 at S831 and S845 is sufficient to lower the threshold for LTP induction, increasing the probability of synaptic plasticity.

glutamate receptor | synapse | CA1 | field recording | patch-clamp recording

It is widely believed that long-lasting changes in synaptic transmission serve as a neural basis of learning and memory. Two such forms of synaptic plasticity, long-term potentiation (LTP) and long-term depression (LTD), have been investigated extensively (1, 2) and proposed as synaptic mechanism of learning and memory (3–5). A key molecular event underlying the expression of LTP at many synapses is delivery of postsynaptic AMPA receptors (AMPARs) to the synaptic surface (6–9). Among the four subunits (GluA1–GluA4) of AMPARs (10, 11), GluA1 has been shown to play an essential role in the expression of LTP in the hippocampus. GluA1 is delivered to postsynaptic spines (12) and functionally incorporated to the synaptic surface (13) upon LTP-inducing stimulation in the CA1 region of hippocampus. In addition, LTP in CA1 of GluA1 knock-out mice is abolished (14), demonstrating the importance of synaptic delivery of GluA1 for the expression of hippocampal LTP.

The C-terminal domains of different AMPAR subunits have diverse structures that include different phosphorylation sites and protein-interacting domains (6–9), which allow subunit-specific regulation of AMPARs during synaptic transmission and plasticity. Among the phosphorylation sites of GluA1, S831 and S845 residues have been investigated most intensively. S831 is phosphorylated by calcium/calmodulin-dependent protein kinase II (CaMKII) or protein kinase C (PKC), while S845 is phosphorylated by cAMP-dependent protein kinase (PKA) (15–17). Functionally, phosphorylation of S831/S845 is involved in the regulation of AMPAR channel properties, such as the modulation of single-channel conductance (18, 19) and channel open probability (20) by S831 and S845, respectively. S831/S845 phosphorylation has also been associated with an increased total (21) and surface (22–24) expression of GluA1. In addition, a number of studies show that S831/S845 phosphorylation is altered by or required for different forms of LTP and LTD as well as learning and memory (25–28). While previous studies have demonstrated that S831/S845 phosphorylation correlates with or is necessary for these various cellular and synaptic functions, there is no evidence that addresses whether S831/S845 phosphorylation alone is sufficient to exert any of these functions.

Here we investigate the role of GluA1 S831/S845 phosphorylation in AMPAR trafficking and synaptic transmission and plasticity in the hippocampus through the analyses of GluA1 S831D/S845D phosphomimetic knock-in mice (GluA1DD mice) (19). GluA1DD mice showed normal total and surface expression and subcellular localization of GluA1 as well as intact basal synaptic transmission. In addition, theta-burst stimulation and spike-timing–dependent plasticity (STDP) protocol with a short pre-post interval, two protocols that were sufficient to induce robust LTP in WT mice, resulted in LTP of similar magnitude in GluA1DD mice. However, GluA1DD mice exhibited LTP induced with 10-Hz stimulation and STDP protocol with a long pre-post interval, neither of which was sufficient to induce LTP in WT mice. These results indicate that phosphorylation of GluA1 at S831 and S845 is sufficient to lower the threshold for LTP induction, highlighting the importance of phosphorylation events at these residues for synaptic plasticity.

Results

Total and Surface Expression as Well as Subcellular Localization of GluA1 Are Intact in GluA1DD Mice. To determine if the basal cellular state of GluA1 is altered in GluA1DD mice, we examined total and surface expression levels of GluA1. Total GluA1 expression was measured from homogenized hippocampi isolated from juvenile WT and GluA1DD mice. Western blot analysis showed no difference in GluA1 level when probed with N-terminal or C-terminal antibody (Fig. 1*A*). GluA2 expression was similarly unaffected in GluA1DD mice (Fig. 1*A*). To examine the surface expression level of GluA1, acute hippocampal slices or dissociated hippocampal cultures prepared from WT and GluA1DD mice were biotinylated to label surface proteins. There was no significant difference in the surface to total ratio of GluA1 in acute hippocampal slices (Fig. 1*B*) or in dissociated hippocampal cultures (Fig. S1). These results indicate that total and surface levels of GluA1 are unchanged in GluA1DD mice.

Author contributions: Y.M. and R.L.H. designed research; Y.M. performed research; Y.M., R.C.J., Y.Y., and K.T. contributed new reagents/analytic tools; Y.M. and R.L.H. analyzed data; and Y.M. and R.L.H. wrote the paper.

Conflict of interest statement: Under a licensing agreement between Millipore Corporation and The Johns Hopkins University, R.L.H. is entitled to a share of royalties received by the University on sales of products described in this article. R.L.H. is a paid consultant to Millipore Corporation. The terms of this arrangement are being managed by The Johns Hopkins University in accordance with its conflict-of-interest policies.

[1]Present address: Department of Integrative Physiology, University of Miyazaki Faculty of Medicine, Miyazaki, Miyazaki 889-1692, Japan.

[2]To whom correspondence should be addressed. E-mail: rhuganir@jhmi.edu.

This article contains supporting information online at www.pnas.org/lookup/suppl/doi:10.1073/pnas.1105261108/-/DCSupplemental.

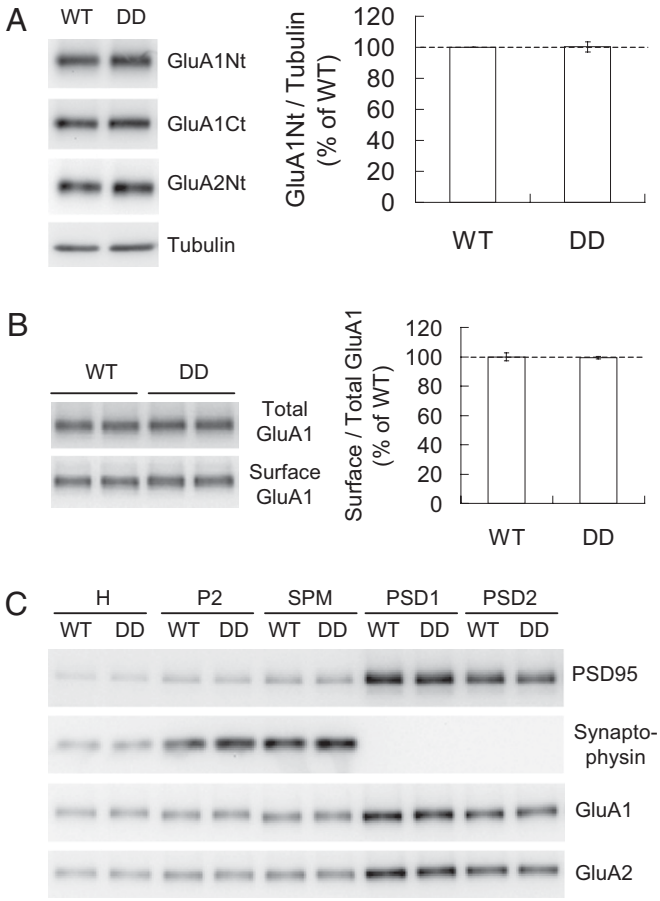

Fig. 1. Total and surface expression as well as subcellular localization of GluA1 are intact in GluA1DD mice. (*A*) Total expression of GluA1. Hippocampi were isolated from juvenile WT and GluA1DD mice and were homogenized. GluA1 was probed by both N-terminal (Nt) and C-terminal (Ct) antibodies, and GluA2 was probed by an N-terminal (Nt) antibody. The signal of the GluA1Nt antibody normalized by tubulin was quantified (WT, 100 ± 0%, n = 3 mice; DD, 100 ± 3%, n = 3 mice; $P > 0.1$). (*B*) Surface expression of GluA1 in acute hippocampal slices. Acute hippocampal slices were biotinylated to label surface proteins. The GluA1 surface/total ratio was quantified (WT, 100 ± 3%, n = 5 slices; DD, 100 ± 1%, n = 5 slices; $P > 0.1$). (*C*) Subcellular localization of GluA1 in vivo. Subcellular fractionation was performed for the hippocampal homogenates taken from WT and GluA1DD mice. Total protein concentration was normalized between WT and GluA1DD samples and among the different fractions. H, homogenate; SPM, synaptosome.

However, this finding does not preclude the possibility that there is a change in the subcellular distribution of GluA1. To examine the GluA1 subcellular localization in vivo, we performed subcellular fractionation of hippocampi taken from WT and GluA1DD mice. Enrichment of the postsynaptic marker PSD95 and absence of the presynaptic marker synaptophysin in postsynaptic density (PSD) fractions demonstrate that postsynaptic proteins were specifically enriched in these fractions (Fig. 1*C*). The levels of GluA1 and GluA2 were similar between WT and GluA1DD mice for PSD fractions as well as all of the other subcellular compartments examined (Fig. 1*C*), demonstrating that GluA1 subcellular localization was normal in GluA1DD mice. To examine the subcellular distribution of GluA1 at the cell surface specifically, we carried out surface immunostaining of GluA1 in hippocampal culture. The surface GluA1 signal was not different between WT and GluA1DD cultures in soma, dendritic shafts, or dendritic spines (Fig. S2), indicating that the subcellular distribution of surface GluA1 is similar between WT and GluA1DD mice. Taken together, these data demonstrate that basal expression and subcellular localization of GluA1 are unaffected in GluA1DD mice.

Basal Synaptic Transmission Is Normal in GluA1DD Mice. Based on our finding that the localization of GluA1 in PSD fractions and at spines is unchanged in GluA1DD mice, it is likely that basal synaptic transmission is also unaffected in these mice. To examine basal synaptic transmission in the CA1 region of hippocampus, we measured miniature excitatory postsynaptic current (mEPSC) by performing whole-cell recordings on the pyramidal cells in CA1 of acute hippocampal slices. There was no significant difference in mEPSC amplitude or frequency between WT and GluA1DD mice (Fig. 2*A*). To examine the synaptic transmission at Schaffer collateral (SC)-CA1 synapses specifically, we recorded the ratio of AMPAR-mediated current to NMDAR-mediated current (AMPA/NMDA ratio) at these synapses. Again, the AMPA/NMDA ratio did not show a significant difference between WT and GluA1DD mice (Fig. 2*B*), indicating that basal synaptic transmission at these synapses is normal in GluA1DD mice.

As an additional index of basal synaptic transmission at SC-CA1 synapses, we examined the input-output (I/O) relationship of field excitatory postsynaptic potentials (fEPSPs) by performing extracellular field recordings at these synapses in acute hippocampal slices. The I/O relationship was determined by plotting fiber volley amplitude against fEPSP slope at different stimulation intensities. The slope of this plot was defined as the I/O slope. There was no significant difference in I/O slope between WT and GluA1DD mice (Fig. 2*C*). Overall, these results indicate that basal synaptic transmission at SC-CA1 synapses is unaffected in GluA1DD mice.

Recent studies demonstrate that the phosphorylation of GluA1 at S845 supports the formation of GluA2-lacking AMPARs (29, 30), suggesting that there are more synaptic GluA2-lacking AMPARs in GluA1DD mice. To test this hypothesis, we examined the effect of NASPM, a selective antagonist of GluA2-lacking AMPARs, on basal synaptic transmission. Continuous perfusion of NASPM for 20 min decreased baseline fEPSP by ∼10% in WT mice. However, this percentage of GluA2-lacking AMPARs was not significantly different between WT and GluA1DD mice (Fig. S3), suggesting that the fraction of GluA2-lacking AMPARs is not altered in GluA1DD mice.

Subthreshold 10-Hz Stimulation Induces LTP in GluA1DD Mice. Although we observed no change in the AMPAR distribution or synaptic transmission at the basal state, it is possible that activity-dependent AMPAR trafficking is altered during synaptic plasticity in GluA1DD mice. To examine a canonical synaptic plasticity, we used field recordings at SC-CA1 synapses to test LTP induced by four trains of theta-burst stimulation. This protocol produced robust and reliable LTP in both WT and GluA1DD mice that was of similar magnitude (Fig. 3*A*), indicating that the ability to induce LTP with suprathreshold stimulation is intact in GluA1DD mice.

However, this experiment would not reveal changes in the threshold for LTP induction. Previous studies have demonstrated that activation of β-adrenergic receptors (βARs) lowers the threshold for LTP such that stimuli that are normally subthreshold for plasticity (e.g., 5–10 Hz) are sufficient to induce LTP, whereas βAR activation does not affect LTP induced by suprathreshold stimulation (e.g., 100-Hz or theta-burst stimulation) (27, 31, 32). Additionally, activation of βARs is reported to increase phosphorylation of GluA1 at S831 or S845, and βAR stimulation fails to facilitate the induction of subthreshould LTP in GluA1 S831A/S845A phosphodeficient mice

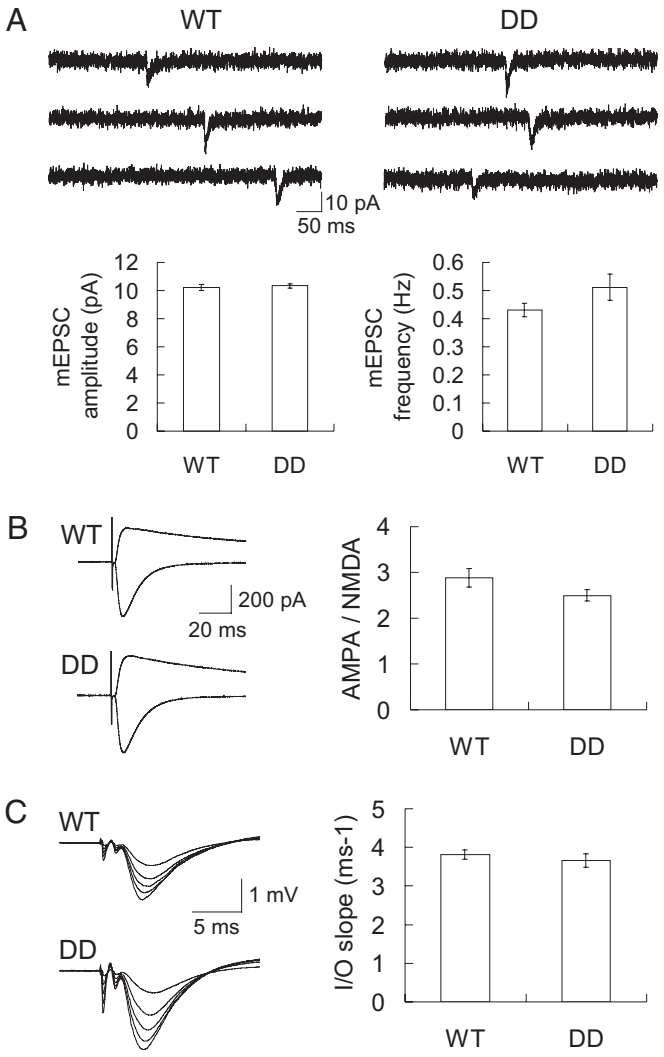

Fig. 2. Basal synaptic transmission is normal in GluA1DD mice. (*A*) mEPSC recordings. Whole-cell voltage-clamp recordings were performed in CA1 pyramidal cells of acute hippocampal slices. Representative traces of the recordings are shown for WT and GluA1DD mice. mEPSC amplitude and frequency were quantified (amplitude: WT, 10.2 ± 0.2 pA, n = 21 cells; DD, 10.3 ± 0.1 pA, n = 22 cells; $P > 0.1$; frequency: WT, 0.43 ± 0.02 Hz, n = 21 cells; DD, 0.51 ± 0.05 Hz, n = 22 cells; $P > 0.1$). (*B*) AMPA/NMDA ratio. EPSCs evoked by the stimulation of Schaffer collateral (SC) were recorded in CA1 pyramidal cells when the cells were held at either −70 mV or +40 mV. Representative EPSC traces at these holding potentials (inward current at −70 mV and outward current at +40 mV) are shown for WT and GluA1DD mice. The peak current intensity at −70 mV was defined as AMPAR current, and the current intensity 50 ms after presynaptic stimulation at +40 mV was defined as NMDAR current. The ratio of AMPAR current to NMDAR current (AMPA/NMDA) was quantified (WT, 2.8 ± 0.2, n = 23 cells; DD, 2.5 ± 0.1, n = 23 cells; $P > 0.1$). (*C*) Input-output relationship. Extracellular field recordings were performed to examine the relationship of fiber volley amplitude and field EPSP (fEPSP) slope at different stimulation intensities. Representative traces for fEPSP at five different stimulation intensities are shown for WT and GluA1DD mice. The slope of fiber volley amplitude against fEPSP slope (I/O slope) was quantified (WT, 3.8 ± 0.2 ms^{-1}, n = 26 slices; DD, 3.7 ± 0.1 ms^{-1}, n = 29 slices; $P > 0.1$).

(27, 28). These findings suggest that phosphorylation of GluA1 S831/S845 reduces the threshold for LTP, and hence it is likely that the threshold for LTP is lower in GluA1DD mice. To address this question, we examined LTP induced with a 10-Hz stimulation. Although this stimulation did not cause any change of synaptic transmission in WT mice, it resulted in long-lasting potentiation in GluA1DD mice (Fig. 3*B*). These results demonstrate that the threshold for LTP induction is reduced in GluA1DD mice.

To confirm that the observed LTP induced with subthreshold stimulation in GluA1DD mice is attributed to the phosphomimicry of GluA1 S831/S845 but not to nonspecific changes in these mice, we examined whether the effect of βAR-induced GluA1 S831/S845 phosphorylation on 10-Hz LTP is occluded in GluA1DD mice. First, we confirmed that a 10-min perfusion of norepinephrine (NE) phosphorylates both S831 and S845 of GluA1 in acute hippocampal slices from WT mice (Fig. 3*C*). We then tested 10-Hz LTP following a 10-min NE perfusion. This protocol induced LTP for both WT and GluA1DD mice, and there was no significant difference in the size of LTP between these mice (Fig. 3*D*). These results confirm that the LTP induced with subthreshold stimulation in GluA1DD mice is a specific effect of aspartate mutations in these mice.

Subthreshold STDP Protocol Induces Potentiation in GluA1DD Mice. Because a subthreshold 10-Hz stimulation resulted in LTP in GluA1DD mice, we questioned whether this represents a general ability of these mice to reduce the threshold for LTP induced by different stimulation protocols. Previous studies have shown that βAR activation shifts the threshold for certain forms of STDP such that subthreshold protocol with a long interval between pre- and postsynaptic stimulations is capable of inducing LTP (28, 33). These observations raise the possibility that subthreshold STDP protocol at a long pre-post interval might result in LTP in GluA1DD mice.

To test this hypothesis, we optimized an STDP protocol (modified from ref. 34) that reliably induced LTP at a short pre-post interval but that produced minimal LTP at a long pre-post interval in CA1 pyramidal cells. In this protocol, one pre-post pairing consisted of a presynaptic stimulation followed at some interval by four action potentials evoked by brief current injections through the patch pipette in the whole-cell current-clamp mode, and this pairing was repeated 100 times at 5 Hz (Fig. 4*A*). This protocol induced robust LTP in WT mice when the pre-post interval was between 5 and 15 ms (Fig. 4*B*). The size of LTP was reduced with a 30-ms interval, and there was only a small transient potentiation that returned back to baseline by ∼10 min with a 50-ms interval (Fig. 4*B*).

From these results, we believed that our STDP protocol with a 50-ms pre-post interval should be weak enough to reveal a shift in the threshold for LTP induction between WT and GluA1DD mice. Consistent with our results of 10-Hz LTP, this weak STDP protocol induced LTP in GluA1DD mice but not in WT mice (Fig. 4*C*). However, in the presence of NE, this STDP protocol induced LTP in both WT and GluA1DD mice that was of similar magnitude (Fig. 4*D*), again confirming that the reduced threshold for LTP induction in GluA1DD mice is a specific effect of the aspartate mutations in these mice. Finally, we found that an STDP protocol with a 5-ms pre-post interval induced similarly robust LTP in WT and GluA1DD mice (Fig. 4*E*), consistent with the idea that phosphorylation of GluA1 at S831 and/or S845 selectively lowers the threshold for LTP induction without affecting the magnitude of LTP induced with suprathreshold stimulation.

Discussion

In this study, we analyzed multiple aspects of synaptic function in GluA1DD mice to examine the roles of GluA1 S831/S845 phosphorylation. GluA1DD mice exhibited LTP induced by two different subthreshold induction protocols, 10-Hz stimulation and STDP protocol with a long (50 ms) pre-post interval. Suprathreshold LTP induction, basal synaptic transmission and basal AMPAR distribution were unaffected in GluA1DD mice.

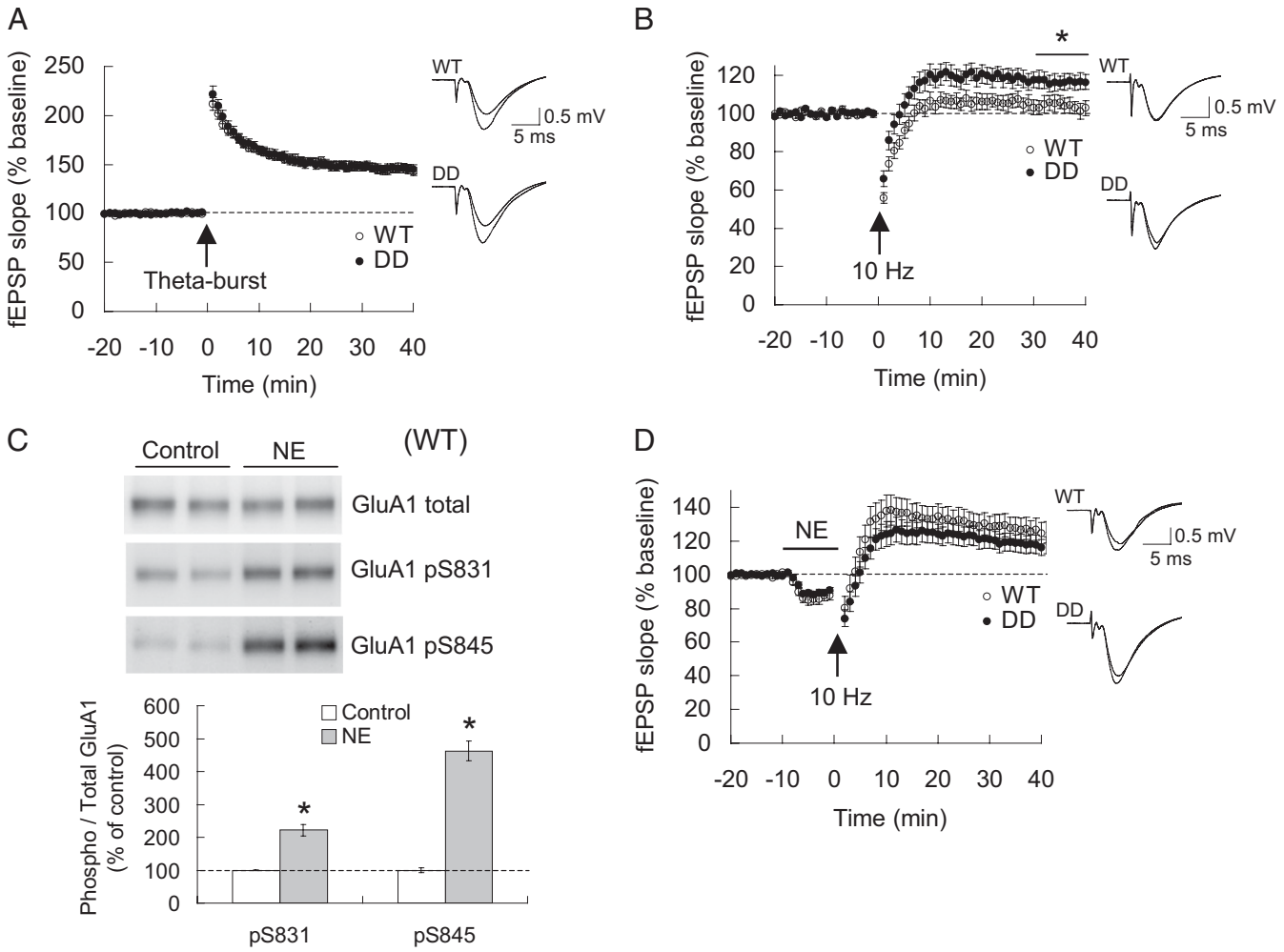

Fig. 3. Subthreshold 10-Hz stimulation induces LTP in GluA1DD mice. (*A*) LTP induced with theta-burst stimulation. Field recordings were performed at SC-CA1 synapses. The percentage of fEPSP slope at 30 to 40 min after the induction of LTP compared with fEPSP slope at baseline (size of potentiation) was quantified (WT, 145 ± 4%, n = 14 slices, $P < 0.001$ from baseline; DD, 146 ± 4%, n = 16 slices, $P < 0.001$ from baseline; $P > 0.1$ between WT and DD). Representative traces of fEPSP at baseline and at 30 to 40 min after LTP induction are shown for WT and GluA1DD mice. (*B*) LTP induced with a 10-Hz stimulation. A continuous 10-Hz stimulation was applied for 90 s (900 pulses in total). The size of potentiation at 30 to 40 min was quantified (WT, 104 ± 4%, n = 10 slices, $P > 0.1$ from baseline; DD, 117 ± 4%, n = 12 slices, $P < 0.005$ from baseline; $P < 0.05$ between WT and DD). Representative fEPSP traces at baseline and at 30 to 40 min are shown. *$P < 0.05$ from WT. (*C*) Phosphorylation of GluA1 S831/S845 by norepinephrine (NE). Ten micromolar NE was perfused for 10 min in acute hippocampal slices prepared from WT mice, and then the slices were chilled and homogenized immediately to measure the phosphorylation level of S831 and S845 with phosphospecific antibodies for each of these sites. The signal of phosphospecific antibodies normalized by total GluA1 was quantified (pS831: Control, 100 ± 1%, n = 4 slices; NE, 221 ± 17%, n = 4 slices; $P < 0.001$; pS845: Control, 100 ± 7%, n = 4 slices; NE, 462 ± 29%, n = 4 slices; $P < 0.001$). *$P < 0.001$ from the control. (*D*) A 10-Hz stimulation with NE perfusion: 10 μM NE was perfused for 10 min, followed by a 10-Hz stimulation for 90 s (900 pulses). The size of potentiation at 30 to 40 min was quantified (WT, 127 ± 7%, n = 12 slices, $P < 0.005$ from baseline; DD, 119 ± 5%, n = 12 slices, $P < 0.005$ from baseline; $P > 0.1$ between WT and DD). Representative fEPSP traces at baseline and at 30 to 40 min are shown.

These results indicate that, although GluA1 S831/S845 phosphorylation is not sufficient to induce LTP on its own, it is sufficient to reduce the threshold for LTP induction.

We propose a model in Fig. S4 to explain the results we obtained. In WT mice, phosphorylation of GluA1 S831/S845 drives extrasynaptic or intracellular GluA1-containing AMPARs to a state in which they can be easily inserted to the synapse by weak stimulation (we call it "readily insertable state"). It is not clear how phosphorylation of GluA1 promotes the transition of AMPARs to this readily insertable state, but one possibility is that GluA1 phosphorylation facilitates the delivery of AMPARs to perisynaptic sites, where they can be easily mobilized into the synapse even when triggered by weak stimulation, resulting in LTP. Indeed, a recent study suggests that phosphorylation of GluA1 S845 might drive GluA1-containing AMPARs to perisynaptic sites (29). This specific targeting may be mediated by changes in the density of negative charges caused by GluA1 S831/S845 phosphorylation, which then increases the interaction of GluA1 with specific scaffolding proteins in the readily insertable microdomain.

In GluA1DD mice, the majority of extrasynaptic GluA1-containing AMPARs might already be in the readily insertable state, thus facilitating insertion of these receptors into the synapse by weak stimulation. In contrast to weak stimulation, which is insufficient to produce LTP unless there is already a pool of AMPARs in the readily insertable state, strong stimulation is capable of both phosphorylating GluA1 (26) and delivering AMPARs from this newly created readily insertable pool to the synapse. This is consistent with our finding that LTP induced with a strong, suprathreshold stimulation is not different between WT and GluA1DD mice. This model is also consistent with our observation of normal basal synaptic transmission and

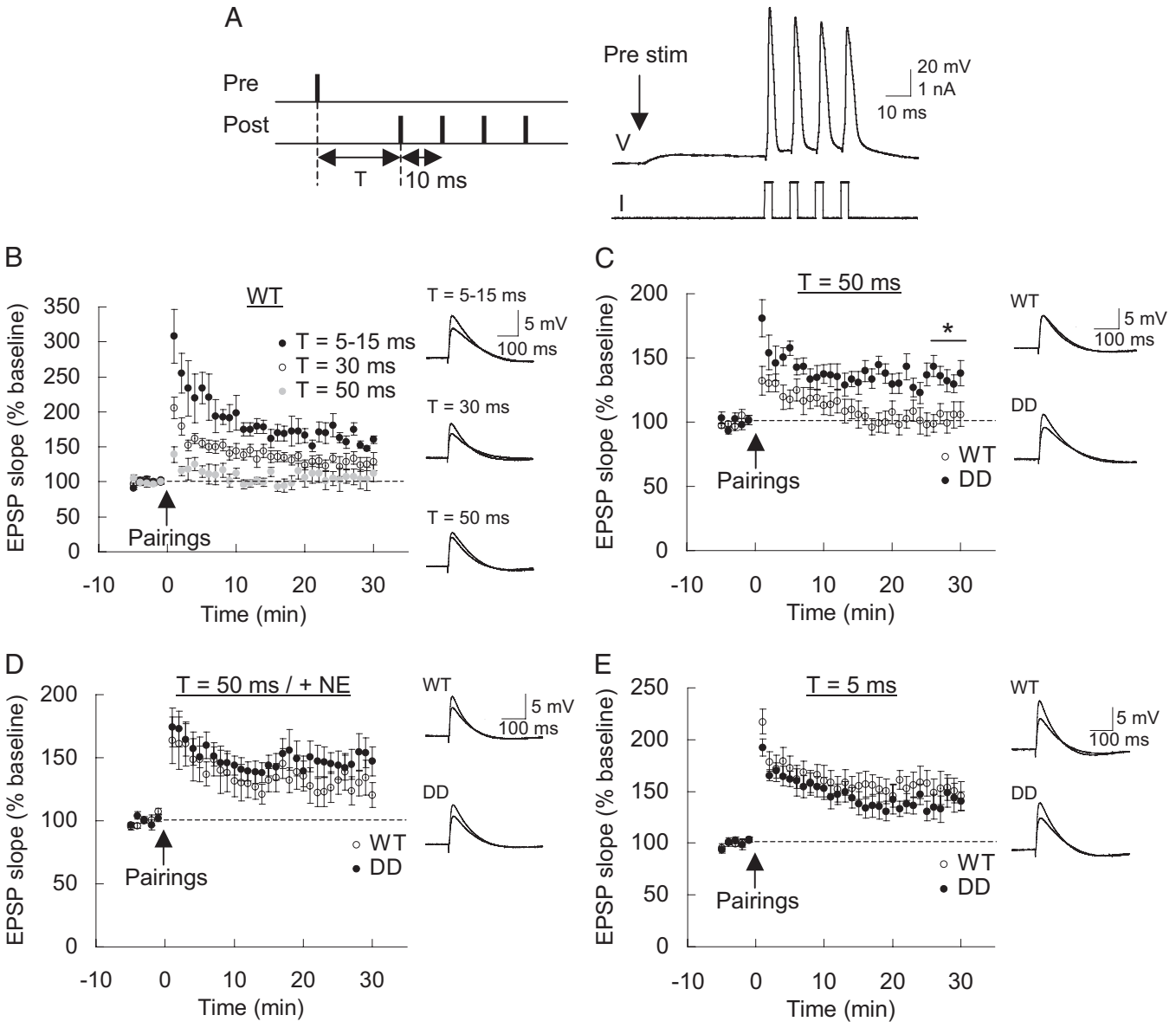

Fig. 4. Subthreshold STDP protocol induces potentiation in GluA1DD mice. (*A*) Schematic diagram of STDP protocol. In this protocol, one pairing consisted of a presynaptic stimulation followed at some interval (T) by four action potentials given at 100 Hz. Each action potential was evoked by a brief injection of high-intensity current with the whole-cell current-clamp mode. This pairing was repeated 100 times at 5 Hz. A representative trace of action potentials (*V*) evoked by current injections (I) is shown. (*B*) STDP in WT mice with different pre-post intervals. STDP protocol was applied with T = 5 to 15 ms, 30 ms, or 50 ms. The percentage of EPSP slope 25 to 30 min after the induction of STDP compared with the EPSP at baseline (size of potentiation) was quantified (5–15 ms, 159 ± 5%, $n = 5$ cells, $P < 0.0005$ from baseline; 30 ms, 128 ± 10%, $n = 6$ cells, $P < 0.05$ from baseline; 50 ms, 107 ± 12%, $n = 6$ cells, $P > 0.1$ from baseline; 5–15 ms vs. 30 ms, $P > 0.1$; 5–15 ms vs. 50 ms, $P < 0.01$; 30 ms vs. 50 ms, $P > 0.1$). Representative traces of EPSP at baseline and at 25 to 30 min after STDP induction are shown for each value of T. (*C*) STDP with 50 ms pre-post interval in WT and GluA1DD mice. The size of potentiation at 25 to 30 min was quantified (WT, 102 ± 8%, $n = 9$ cells, $P > 0.1$ from baseline; DD, 136 ± 8%, $n = 8$ cells, $P < 0.005$ from baseline; $P < 0.01$ between WT and DD). Representative EPSP traces at baseline and at 25 to 30 min are shown for WT and GluA1DD mice. *$P < 0.01$ from WT. (*D*) STDP with 50 ms pre-post interval with NE perfusion in WT and GluA1DD mice. Ten micromolars of NE was perfused for the entire period of experiments. The size of potentiation at 25 to 30 min was quantified (WT, 130 ± 11%, $n = 9$ cells, $P < 0.05$ from baseline; DD, 148 ± 11%, $n = 10$ cells, $P < 0.005$ from baseline; $P > 0.1$ between WT and DD). Representative EPSP traces at baseline and at 25 to 30 min are shown. (*E*) STDP with 5 ms pre-post interval in WT and GluA1DD mice. The size of potentiation at 25 to 30 min was quantified (WT, 152 ± 13%, $n = 9$ cells, $P < 0.005$ from baseline; DD, 139 ± 11%, $n = 7$ cells, $P < 0.05$ from baseline; $P > 0.1$ between WT and DD). Representative EPSP traces at baseline and at 25 to 30 min are shown.

cellular distribution of GluA1 in GluA1DD mice, because the lateral movement of AMPARs from extrasynaptic to perisynaptic surface would not change any of these measurements.

Previously, phosphorylation of GluA1 S831/S845 has been associated with a larger total (21) and surface (22–24) expression of GluA1. Although these observations are not consistent with our results, there are a number of factors that could account for these differences. Some previous studies are simply reporting a correlation between GluA1 phosphorylation and surface GluA1 level (22, 23). Others have examined the causal effect of GluA1 phosphorylation by using an overexpression system in dissociated culture or organotypic hippocampal slices (21, 24), which has a clear disadvantage in that the expression level and subunit composition of overexpressed receptors are substantially different from those

of endogenous receptors and that the receptors are measured in a less physiologically intact system. We believe that our study, which measured the functional changes induced by phosphomimetic mutations on endogenous GluA1 in acute hippocampal slices or from an in vivo sample, is more suitable for examining causal effect of GluA1 S831/S845 phosphorylation in the physiological context.

Previous studies have shown that phosphorylation of GluA1 S831/S845 leads to the enhancement of learning and memory (26, 27). In future studies it will be interesting to examine whether learning and memory is enhanced in the GluA1DD mice.

Materials and Methods

Mice. Approximately 3- to 4-wk-old WT and GluA1DD (homozygous) mice with 129 and C57BL/6 hybrid genetic background were used for all experiments. See *SI Materials and Methods* for details.

Surface Biotinylation. Hippocampal slices (400-μm thick) were prepared and were subjected to biotinylation to label surface proteins. See *SI Materials and Methods* for details.

Subcellular Fractionation. Hippocampi were isolated and homogenized, followed by the extraction of P2, synaptosome (SPM) and two PSD fractions. See *SI Materials and Methods* for details.

Whole-Cell Recordings. Whole-brain coronal slices (300-μm thick) were prepared, on which whole-cell recordings were performed for CA1 pyramidal cells. mEPSC and AMPA/NMDA ratio were recorded in voltage-clamp mode, and STDP experiments were performed in current-clamp mode. See *SI Materials and Methods* for details.

Extracellular Field Recordings. Hippocampal slices (400-μm thick) were prepared, on which extracellular field recordings were performed. The field potentials at CA1 stratum radiatum evoked by the stimulation of SC were recorded. See *SI Materials and Methods* for details.

ACKNOWLEDGMENTS. We thank Dr. Lenora Volk and Dr. Jean-Claude Béïque for excellent technical support, Dr. Victor Anggono for critical reading of the manuscript, and all the other R.L.H. laboratory members for their assistance and invaluable comments. This work was supported by Grants R01 NS036715 and R01 MH064856 from the National Institutes of Health (to R.L.H.) and a predoctoral fellowship from the Nakajima Foundation (to Y.M.). R.L.H. is an investigator of the Howard Hughes Medical Institute.

1. Malenka RC, Nicoll RA (1999) Long-term potentiation—A decade of progress? *Science* 285:1870–1874.
2. Malenka RC, Bear MF (2004) LTP and LTD: An embarrassment of riches. *Neuron* 44:5–21.
3. Martin SJ, Grimwood PD, Morris RG (2000) Synaptic plasticity and memory: An evaluation of the hypothesis. *Annu Rev Neurosci* 23:649–711.
4. Martin SJ, Morris RG (2002) New life in an old idea: The synaptic plasticity and memory hypothesis revisited. *Hippocampus* 12:609–636.
5. Lynch MA (2004) Long-term potentiation and memory. *Physiol Rev* 84:87–136.
6. Song I, Huganir RL (2002) Regulation of AMPA receptors during synaptic plasticity. *Trends Neurosci* 25:578–588.
7. Malinow R, Malenka RC (2002) AMPA receptor trafficking and synaptic plasticity. *Annu Rev Neurosci* 25:103–126.
8. Bredt DS, Nicoll RA (2003) AMPA receptor trafficking at excitatory synapses. *Neuron* 40:361–379.
9. Shepherd JD, Huganir RL (2007) The cell biology of synaptic plasticity: AMPA receptor trafficking. *Annu Rev Cell Dev Biol* 23:613–643.
10. Hollmann M, Heinemann S (1994) Cloned glutamate receptors. *Annu Rev Neurosci* 17: 31–108.
11. Dingledine R, Borges K, Bowie D, Traynelis SF (1999) The glutamate receptor ion channels. *Pharmacol Rev* 51:7–61.
12. Shi SH, et al. (1999) Rapid spine delivery and redistribution of AMPA receptors after synaptic NMDA receptor activation. *Science* 284:1811–1816.
13. Hayashi Y, et al. (2000) Driving AMPA receptors into synapses by LTP and CaMKII: Requirement for GluR1 and PDZ domain interaction. *Science* 287:2262–2267.
14. Zamanillo D, et al. (1999) Importance of AMPA receptors for hippocampal synaptic plasticity but not for spatial learning. *Science* 284:1805–1811.
15. Roche KW, O'Brien RJ, Mammen AL, Bernhardt J, Huganir RL (1996) Characterization of multiple phosphorylation sites on the AMPA receptor GluR1 subunit. *Neuron* 16: 1179–1188.
16. Mammen AL, Kameyama K, Roche KW, Huganir RL (1997) Phosphorylation of the alpha-amino-3-hydroxy-5-methylisoxazole4-propionic acid receptor GluR1 subunit by calcium/calmodulin-dependent kinase II. *J Biol Chem* 272:32528–32533.
17. Barria A, Derkach V, Soderling T (1997) Identification of the Ca2+/calmodulin-dependent protein kinase II regulatory phosphorylation site in the alpha-amino-3-hydroxyl-5-methyl-4-isoxazole-propionate-type glutamate receptor. *J Biol Chem* 272: 32727–32730.
18. Derkach V, Barria A, Soderling TR (1999) Ca2+/calmodulin-kinase II enhances channel conductance of alpha-amino-3-hydroxy-5-methyl-4-isoxazolepropionate type glutamate receptors. *Proc Natl Acad Sci USA* 96:3269–3274.
19. Kristensen AS Mechanism of CaMKII regulation of AMPA receptor gating. *Nat Neurosci*, in press.
20. Banke TG, et al. (2000) Control of GluR1 AMPA receptor function by cAMP-dependent protein kinase. *J Neurosci* 20:89–102.
21. Kessels HW, Kopec CD, Klein ME, Malinow R (2009) Roles of stargazin and phosphorylation in the control of AMPA receptor subcellular distribution. *Nat Neurosci* 12: 888–896.
22. Ehlers MD (2000) Reinsertion or degradation of AMPA receptors determined by activity-dependent endocytic sorting. *Neuron* 28:511–525.
23. Oh MC, Derkach VA, Guire ES, Soderling TR (2006) Extrasynaptic membrane trafficking regulated by GluR1 serine 845 phosphorylation primes AMPA receptors for long-term potentiation. *J Biol Chem* 281:752–758.
24. Man HY, Sekine-Aizawa Y, Huganir RL (2007) Regulation of alpha-amino-3-hydroxy-5-methyl-4-isoxazolepropionic acid receptor trafficking through PKA phosphorylation of the Glu receptor 1 subunit. *Proc Natl Acad Sci USA* 104:3579–3584.
25. Lee HK, Barbarosie M, Kameyama K, Bear MF, Huganir RL (2000) Regulation of distinct AMPA receptor phosphorylation sites during bidirectional synaptic plasticity. *Nature* 405:955–959.
26. Lee HK, et al. (2003) Phosphorylation of the AMPA receptor GluR1 subunit is required for synaptic plasticity and retention of spatial memory. *Cell* 112: 631–643.
27. Hu H, et al. (2007) Emotion enhances learning via norepinephrine regulation of AMPA-receptor trafficking. *Cell* 131:160–173.
28. Seol GH, et al. (2007) Neuromodulators control the polarity of spike-timing-dependent synaptic plasticity. *Neuron* 55:919–929.
29. He K, et al. (2009) Stabilization of Ca2+-permeable AMPA receptors at perisynaptic sites by GluR1-S845 phosphorylation. *Proc Natl Acad Sci USA* 106:20033–20038.
30. Clem RL, Huganir RL (2010) Calcium-permeable AMPA receptor dynamics mediate fear memory erasure. *Science* 330:1108–1112.
31. Thomas MJ, Moody TD, Makhinson M, O'Dell TJ (1996) Activity-dependent beta-adrenergic modulation of low frequency stimulation induced LTP in the hippocampal CA1 region. *Neuron* 17:475–482.
32. Katsuki H, Izumi Y, Zorumski CF (1997) Noradrenergic regulation of synaptic plasticity in the hippocampal CA1 region. *J Neurophysiol* 77:3013–3020.
33. Lin YW, Min MY, Chiu TH, Yang HW (2003) Enhancement of associative long-term potentiation by activation of beta-adrenergic receptors at CA1 synapses in rat hippocampal slices. *J Neurosci* 23:4173–4181.
34. Wittenberg GM, Wang SS (2006) Malleability of spike-timing-dependent plasticity at the CA3-CA1 synapse. *J Neurosci* 26:6610–6617.